Chitosan Derivatives as Dynamic Coatings for Transferrin Glycoform Separation in Capillary Electrophoresis

Nadia Maria Porpiglia[1,‡], Irene Tagliaro[2,‡], Beatrice Pellegrini[2,3], Arianna Alessi[2,3], Franco Tagliaro[1,4,], Laura Russo[5,6], Francesca Cadamuro[5], Giacomo Musile[1], Carlo Antonini[2*], Sabrina Bertini[3*].*

[1] Unit of Forensic Medicine, Department of Diagnostics and Public Health, University of Verona, Verona, Italy. Address: Piazzale L. A. Scuro, 10 - 37134 Verona (VR) Italy, Telephone number: (+39) 0458124618, Fax number: (+39) 0458027623, nadia.porpiglia@univr.it (N.P.), giacomo.musile@univr.it (G.M.), franco.tagliaro@univr.it (F.T.).

[2] Department of Materials Science, University of Milano - Bicocca, Milano, 20125 Milan, Italy; Telephone number (+39) 0264485188, carlo.antonini@unimib.it (C.A.); irene.tagliaro@unimib.it (I.T.).

[3] Istituto di Ricerche Chimiche e Biochimiche G. Ronzoni, Carbohydrate Science Department, 20133 Milan, Italy; alessi@ronzoni.it (A.A.); bertini@ronzoni.it (S.B.); pellegrini@ronzoni.it (B.P.)

[4] Institute Translational Medicine and Biotechnology, Sechenov First Moscow State Medical University, Address: 2-4 Bolshaya Pirogovskaya Street, 119991 Moscow, Russia.

[5] Department of Biotechnology, University of Milano - Bicocca, Milano, 20125 Milan, Italy; Telephone Number (+39) 0264483462, laura.russo@unimib.it (L.R.); f.cadamuro@campus.unimib.it (F.C.);

[6] CÚRAM SFI Research Centre for Medical Devices, National University of Ireland Galway, H92 W2TY, Ireland (L.R.)

‡ Nadia Maria Porpiglia and Irene Tagliaro contributed equally to this work

* corresponding authors: franco.tagliaro@univr.it, carlo.antonini@unimib.it, bertini@ronzoni.it

KEYWORDS. Chitosan derivative, capillary electrophoresis, dynamic coating, carbohydrate deficient transferrin.

ABSTRACT. Chitosan and its derivatives are interesting biopolymers for different field of analytical chemistry, especially in separation techniques. The present study was aimed at testing chitosan water soluble derivatives as dynamic coating agents for application to capillary electrophoresis. In particular, chitosan was modified following three different chemical reactions (nucleophilic substitution, reductive amination, and condensation) to introduce differences in charge and steric hindrance, and to assess the effect of these physico-chemical properties in capillary electrophoresis. The effects were tested on the capillary electrophoretic separation of the glycoforms of human transferrin, an important iron-transporting serum protein, one of which, namely disialo-transferrin (CDT), is a biomarker of alcohol abuse. Chitosan derivatives were characterized by using NMR and ^{1}H NMR, HP-SEC-TDA, DLS, and rheology. The use of these compounds as dynamic coatings in the electrolyte running buffer in capillary electrophoresis was tested assessing the peak resolution of the main glycoforms of human transferrin and particularly of disialo-transferrin. The results showed distinct changes of the peak resolution produced by the different derivatives. The best results in terms of peak resolution were achieved using polyethylene glycol (PEG)-modified chitosan, which, in comparison to a reference analytical approach, provided an almost baseline resolution of disialo-transferrin from the adjacent peaks.

INTRODUCTION

The application of chitosan-based materials in analytical chemistry has attracted increasing interest [1]. Chitosan (Ch) is the deacetylated form of chitin, one of the most abundant natural biopolymers [2]: it has excellent properties that include biocompatibility, great adsorption capability and adhesiveness [3,4]. Due to these characteristics, chitosan has been applied in different fields of analytical chemistry, e.g. as stationary material of chromatographic columns [5], as adsorption material for concentration and extraction purposes [6,7], and as enzyme-immobilizing matrix [8,9]. Chitosan properties strongly depend on the degree of acetylation (DA) [10], on the acetyl group distribution, and on the molecular weight. Its main reactive functional groups are hydroxyl (OH) and amine (NH_2) groups which impart to Ch a cationic nature, due to the protonation of amine in acidic medium, enhancing the interaction with negatively charged molecules (e.g. fatty acids, metal ions, proteins, and macromolecules) [3]. Thanks to its hydroxyl and amine moieties, Ch can be modified easily to introduce specific functional groups for obtaining the desired interactions with analytes. The functionality modification also allows to overcome the Ch lack of solubility: pristine Ch is soluble only in acidic conditions due to the protonation of the amine group.

An analytical technique which can potentially benefit from the use of modified chitosan is capillary electrophoresis (CE). This relatively new separation technique combines electrophoretic/electrokinetic separation principles with an instrumental design that mimics liquid chromatography. The main strengths of CE include: (i) short analysis times, (ii) low sample and reagent consumption, (iii) low waste production and (iv) low running costs [11,12]. A key feature of CE is the flexibility of implementing several detection modes, such as UV-Vis, fluorescence, conductimetry and mass spectrometry [13,14]. Such flexibility opens up a broad field of analysis ranging from inorganic ions to drugs, peptides, proteins and virus particle [15–19]. In CE, separation occurs inside narrow-bore fused-silica capillaries (20–100 μm I.D., 20–100 cm length), which, on one side, limit band broadening but, on the other side, because of a high surface-to-volume ratio, may lead to adsorption of analytes onto the capillary walls. These secondary interactions [20] may exert spurious effects both on proper electrophoretic phenomena, e.g., pseudo-ion exchange chromatography on the inner surface of the capillary, as well as on the electroendosmotic flow (EOF), responsible for inconsistency of the migration times and of peak resolution [11]. Several approaches have been adopted in the past to control adsorption onto the capillary wall, including the use of separation buffers at low pH and high ionic strength, or special additives that interact reversibly with the silica wall. Other approaches include the chemical modification of the capillary wall with neutral or charged

molecules [21–25]. Studies conducted in reversed EOF investigated the effect of non-modified chitosan for the separation of drugs and inorganic ions [26–28], while derivatized chitosan (i.e. especially methyl and carboxymethyl) showed interesting application perspectives for the separation of proteins [29–31]. Although many efforts have been made in this direction, analyte adsorption, and particularly protein adsorption, is still an open critical issue in several CE applications, also in the presence of additives able to lower interaction with the capillary wall. Analyte adsorption remains critical for the analysis of carbohydrate-deficient transferrin (CDT), one of the most used biomarkers of chronic alcohol abuse, adopted in clinical and non-clinical contexts (e.g., driving and weapon license certification, occupational health, child custody eligibility etc.) [32]. The term CDT is the collective name of a group of the less glycosylated glycoforms of the iron-transporting protein hTf, and specifically of disialo-hTf [33]. Its analysis requires the resolution of the different hTf glycoforms, from asialo-hTf to hexasialo-hTf (characterized by different glycosylation degrees), with the final aim of measuring the relative percentage area of disialo-hTf (P_2) (Figure 1) [34].

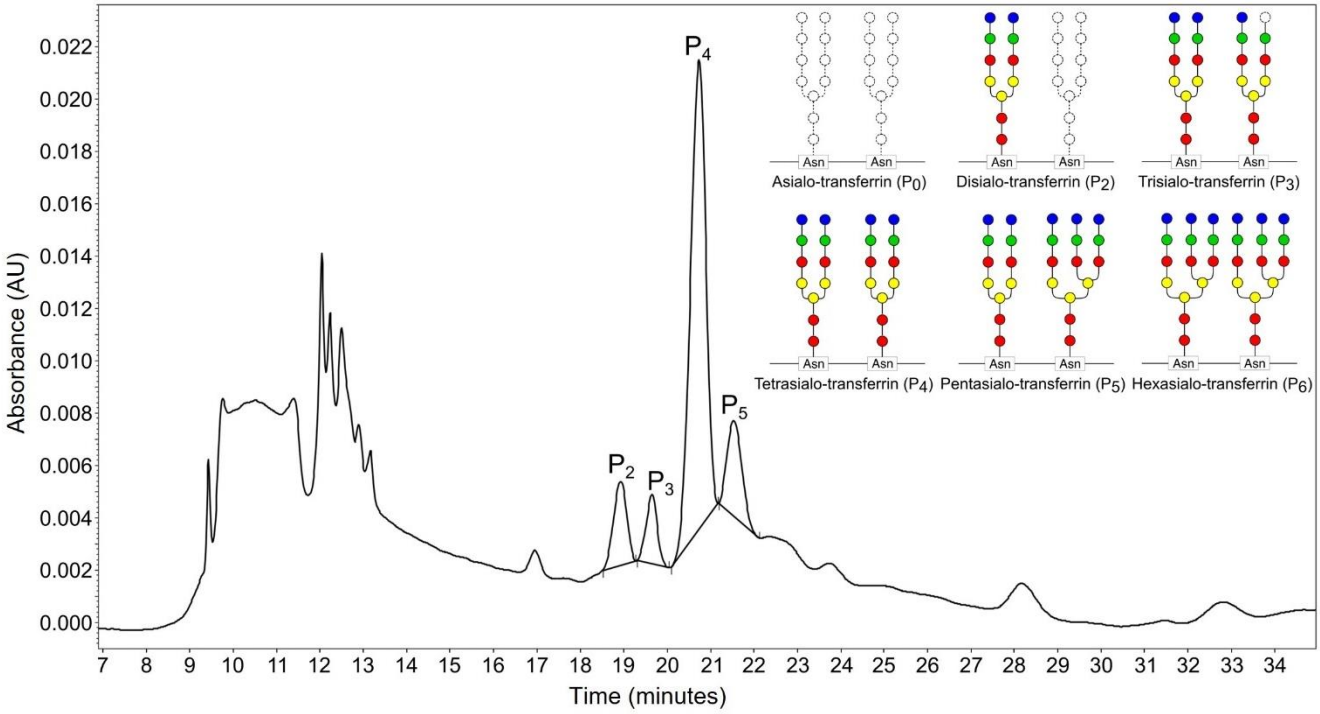

Figure 1. Electropherogram of CDT analysis performed with traditional running buffer with schematic representation of the glycoforms of human transferrin (hTf) involved in the forensic analysis of CDT: disialo-hTf (P2) to pentaasialo-hTf (P5). The crowd of peaks migrating between 9 and 14 minutes correspond to gamma globulins and other endogenous UV absorbing-material (%CDT = 13.36% of total Tf). Symbol legend: Asn = asparagine residue; red circle = N-acetylglucosamine; yellow circle = mannose; green circle = galactose; blue circle = sialic acid. AU = absorbance units at 200 nm wavelength.

Despite a well-established use of CE for CDT determination, the separation of hTf glycoforms is hindered by the natural tendency of these molecules to interact with the fused-silica capillary walls. To overcome this problem, the most common approach is based on the addition of a cationic additive (1-4 diamine butane, DAB) in the separation running buffer (borate, at alkaline pH) to passivate the ionized silanols responsible of spurious interactions of the serum protein, also known “dynamic coating” [35]. The term dynamic coating refers to the presence in the running buffer of an agent which, by reversible ionic interactions, hinders the analyte binding to the capillary wall. The action of the dynamic coating determines the shielding of the inner capillary surface to allow an efficient electrophoretic separation of CDT by suppression of spurious interactions of the serum proteins, which may introduce undesired parasitical

separation mechanisms. For the same purpose, in other studies [36,37], attempts have been made by applying cellulose derivatives as dynamic coatings; however, the results did not meet the required sensitivity (i.e. signal-to-noise ratio) and specificity (due to UV absorption of cellulose) for clinical use because of interference from the matrix. For this reason, CDT determination in serum required laborious immunoextraction prior to electrophoretic separation.

Besides the above-mentioned studies, the use of modified chitosan has never been reported in the literature. On these grounds, in the present study, we aimed at exploring the potential application of chitosan derivatives as a new class of additives acting as novel form of dynamic coating to optimize the separation of hTf glycoforms.

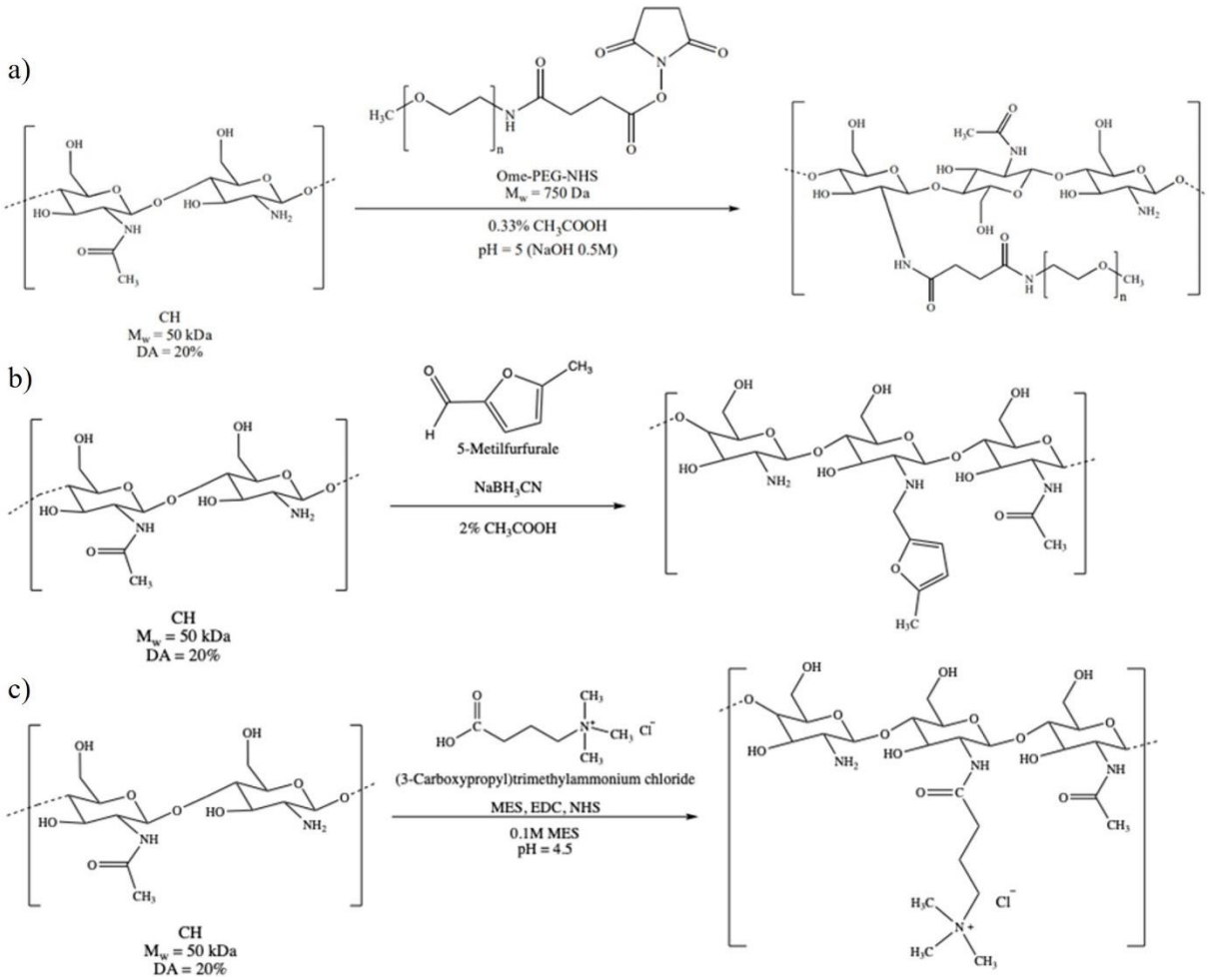

Figure 2. Representation of the different Ch derivatives: a) Ch-Ome-PEG; b) Ch-MF; c) Ch-QA.

Three different Ch derivatives were synthetized as reported in Figure 2. A PEG-modified Ch (Ch-Ome-PEG) was prepared by nucleophilic substitution employing an NHS activated PEG (Figure 2, a), a methyl furan Ch (Ch-MF) was synthetized by reductive amination with methyl furfural (Figure 2, b), and finally a quaternary Ch (Ch-QA) by carbodiimide condensation with a quaternary ammonium linker (Figure 2, c). Ch derivatives were first characterized employing complementary techniques to investigate the material properties. In particular, Nuclear Magnetic Resonance Spectroscopy (NMR) was applied to elucidate the molecular structure and Dynamic Light Scattering (DLS) was used to determine the Hydrodynamic Radius and Zeta Potential. On these grounds, a comparative study of the Ch derivative performances was conducted by testing the resolution of the hTf glycoforms essential for CDT determination, including real

serum samples. This study should be considered propaedeutic to the development of a new CE method for CDT analysis taking advantage of this innovative capillary coating agent.

MATERIALS AND METHODS

Materials

Methoxy-PEG (Ome-PEG-NHS), 5-methyl furfural (MF), 3-carboxypropil trimethyl ammonium chloride, 2-(N-morpholino) ethane sulfonic acid (MES), 1- Ethyl-3-(3-dimethylaminopropyl)carbodiimide (EDC), N-Hydroxysuccinimide (NHS), glacial acetic acid (≥ 99.9%), chloride acid, sodium chloride, sodium acetate, sodium hydroxide, sodium azide and 1-4 diamino butane (DAB) was purchased from Sigma-Aldrich Co. (Steinheim, Germany). Sodium cyanoborohydride ($NaBH_3CN$) was from Fluka (Munich, Germany), and boric acid from Amersham Pharmacia Biotech AB (Staffanstorp, Sweden). Deionized water was obtained by Culligan System (Rosemont, IL, USA) and Deuterated water by Cortecnet (Paris, France). All materials used were of analytical grade. To calibrate HP-SEC-TDA, a pullulan (PolyCAL-Pul86k) purchased by Malvern Panalytical Instruments (Malvern, United Kingdom) was used. Low molecular weight Chitosan (Ch) was obtained from Carbosynth Ltd (Compton, United Kingdom). The CDT test solution (used for the CE analyses) was purchased from Recipe (Munich, Germany).

Synthesis

Three types of syntheses were performed to achieve chemical modifications, i.e.: (i) nucleophilic substitution, (ii) reductive amination and (iii) condensation. The products of these chemical reactions were named Ch-Ome-PEG, Ch-MF, Ch-QA, respectively.

For the nucleophilic reaction (i), Ch (about 60 mg) was dissolved in 3 mL of 0.33% acetic acid solution, mixed by sonication, vortexed until homogeneous solution and finally stirred at room temperature for 24 h. In previous works, Ch was solubilized in organic solvent [33,38] or more concentrated acetic acid [39]. In this work, we investigated alternative routes to reduce Ome-PEG-NHS hydrolysis: before adding the reagent, Ch solution was adjusted to pH 5 with a 0.5 M NaOH solution.

Considering a molar ratio of 1:1 Ch:Ome-PEG-NHS, about 0.25 g of Ome-PEG-NHS were solubilized in 2 mL of milli-Q water. The solution was dialyzed in 0.3 M AcONa/0.5 M NaCl solution for three days, and in milli-Q water for other five days, using a 3.5 kDa and/or 12-14 kDa dialysis membranes. The modified Ch was purified through filtration using membrane filters. The solution was concentrated with a rotavapor and freeze-dried for characterization.

For the reductive amination reaction (ii), previously reported reaction between Ch and methyl furfural (MF) was performed [40]. Briefly, Ch (1.2 g) was dissolved in 35 mL of 2% acetic acid solution, mixed by sonication, vortexed until a homogeneous solution was obtained and finally stirred at room temperature for 24 h. Then, 206 µL of MF were added to the dissolved chitosan, and the solution was left under gentle stirring for 30 min. Afterwards, 0.065 g of sodium cyanoborohydride were added, and the reaction solution was stirred for 3 h at room temperature. The solution was dialyzed against 0.01 M sodium chloride solution for 1 day, and in milli-Q water for other five days, using 3.5 kDa dialysis membranes at 40°C. The solution was concentrated with rotavapor and freeze-dried for characterization.

For the condensation reaction (iii), Ch (about 1 g) was dissolved in 20 mL of 0.1 M MES (pH 4.5), mixed by sonication, vortexed until a homogeneous solution was obtained and finally stirred at room temperature for 24 h. The reactive 3-carboxypropil trimethyl ammonium chloride (about 0.2 g) was solubilized in 10 mL of 0.1 M MES (pH 4.5). Then, EDC (1 g) and NHS (0.6 g) were added to the reactive solution and stirred for 30 minutes. Finally, this solution was added to Ch. The solution was dialyzed against 6%

sodium chloride solution for 1 day, and in milli-Q water for a further five days, using 3.5 kDa dialysis membranes. The solution was concentrated with rotavapor and freeze-dried for the characterization.

NMR

To ensure an appropriate resolution, approximately 7 mg of Ch samples were solubilized in 600 µL of deuterated hydrochloric acid and transferred into a 5 mm NMR tube. Proton spectra were acquired with pre-saturation of residual HDO, at 303K, using 24 scans, 12 s relaxation delay, and a number of time-domain points equal to 32k. COSY spectra were acquired with pre-saturation of residual HDO, at 303K, using 20 scans, 2 s relaxation delay, and a time-domain equal to 2048 x 256. HSQC-dept spectra were acquired with pre-saturation of residual HDO, at 303K, using 20 scans, 2 s relaxation delay, a time-domain 2048 x 256 and 1JC-H 150 Hz. All derivatives spectra were acquired on a Bruker Avance HD NMR spectrometer (Bruker, Karlsruhe, Germany), operating at 500 MHz and using a BBO Probe while Ch spectra were acquired on a Bruker Avance NEO NMR spectrometer (Bruker, Karlsruhe, Germany), operating at 500 MHz and using a CRIO Probe. All spectra were elaborated with the TopSpin software (v. 4.1.1).

The signals were calibrated assigning 300 to the integral of the signal related to the methyl group of acetyl (Ac). The degree of substitution (DS%), reported in Table 1, was evaluated using the following equation:

Eq.1

$$\mathrm{DS}(\%)_{\mathrm{Ch-Ome-PEG}} = \frac{\frac{\mathrm{OAc}}{3}}{(1\mathrm{A}, 1\mathrm{D}, 1\mathrm{R}) + \frac{\mathrm{Ac}}{3}}$$

$$\mathrm{DS}(\%)_{\mathrm{Ch-MF}} = \frac{2\mathrm{R}}{2\mathrm{D} + 2\mathrm{R} + \frac{\mathrm{Ac}}{3}}$$

$$\mathrm{DS}(\%)_{\mathrm{Ch-QA}} = \frac{\frac{\mathrm{N^{+}(Ac)_3}}{9}}{(1\mathrm{A}, 1\mathrm{D}, 1\mathrm{R}) + \frac{\mathrm{Ac}}{3}}$$

In Eq 1 Ac is the integral value peak at around 2.1 ppm, (1A,1D, 1R) is the sum of anomeric proton corresponding to acetylated, deacetylated and substituted units (4.6ppm-4.7ppm), 2D is the integral value of H2 of deacetylate unit and 2R is the integral value of H2 of substituted unit.

DLS

Dynamic Light Scattering (DLS) was performed using the Zetasizer Nano ZS (Malvern, United Kingdom) with a fixed scattering angle of 173° and a 633-nm helium–neon laser. Data were analyzed using Zetasizer software version 7.11 (Malvern, United Kingdom). For size analyses, solutions of 1 mg/mL were prepared solubilizing Ch derivatives in 0.3 M sodium acetate pH 8 and Ch in 0.3 M sodium acetate/0.3 M acetic acid. For Zeta Potential (Zp) analyses, starting stock solutions of 2 mg/mL were prepared by solubilizing Ch derivatives in water and Ch in 0.3 M sodium acetate /0.3 M acetic acid. These solutions were then diluted in water to the following concentrations: 1 mg/mL, 0.5 mg/mL, 0.2 mg/mL and 0.1 mg/mL. Each solution concentration was filtered with a 0.22 µm Syringe Filter made of cellulose acetate and analyzed at 25°C with automatic measurement. Disposable polystyrene ZEN0040 and DTS1070 cuvettes were used

for size and Zp measures, respectively. The molecular weight was calculated by the Stokes-Einstein equation.

CE analysis

The analysis of CDT was performed using a model PA 800 plus capillary electrophoresis system equipped with a UV-DAD detector (Beckman Coulter, Brea, CA, USA). The evaluation of the capillary surface ionization was performed through the measurement of the so-called streaming potential (SP) on a Capel-205 electropherograph (Lumex, Fraserview Pl, BC, Canada), specifically equipped with a dedicated module.

Data acquisition and processing were carried out using the PA 800 plus 32 Karat software for separation, electrophoretic parameters and %CDT determination, and with Elforun 205 for the streaming potential determination.

The reference method used for CDT analysis (named "traditional method") is concisely described as follows: separation occurred in an uncoated fused-silica capillary of 50 µm i.d. and 60 cm total length (50 cm from the injection end to the detection window) at a voltage of 25 kV in 120 mM borate buffer containing 6 mM DAB, pH 8. The capillary cartridge temperature was maintained at 25°C. In the last experiment, a capillary with 30 µm i.d. x 60 cm total length (50 cm to the detection window) was used with the same running buffer composition. Because of a higher electrical resistance, the separation voltage was increased to 30 kV for this particular analysis. The wavelength of detection is set at 200 nm. A commercially available serum CDT test solution (consisting of a stabilized pool of sera of alcoholic patients) was used as the test sample and injected by positive pressure at 3.5 kPa for 25 s. Prior to each run, the capillary was sequentially rinsed with: (i) 0.1 M NaOH, (ii) 0.5 M borate at pH 8, and (iii) running buffer, at 345 kPa for 3 min each (9 min total). The capillary was also rinsed each day of use, before every analytical session, with: (i) 1 M NaOH, (ii) deionized water, (iii) 0.5 M borate at pH 8, and (iv) running buffer at 345 kPa, for 5 min for each solution (20 min total). In the present study, Ch derivatives were, in turn, added to the running buffer at different concentrations. The reference method, also referred as traditional method, does not contain Ch derivatives.

The resolution between the peaks was determined by the following equation:

Eq. 2

$$R = \frac{2.0\ (Mt_2 - Mt_1)}{(W_2 + W_1)}$$

where Mt values correspond to the peak migration times and W to the peak widths at the baseline, and the subscripts 1 and 2 refer to the two peaks of interest (specifically for our study: disialo-hTf, P_2, trisialo-hTf, P_3, Figure 1). The concentration of CDT (P2) was calculated from the integration of the electropherogram peak area, as: P2 peak area/ $\sum$ Tf peak area x 100.

RESULTS AND DISCUSSION

A multi-technique characterization of Ch derivatives was conducted, to measure physico-chemical properties (i.e., steric hindrance, charge, viscosity) and subsequently correlate them to the effects observed in hTf glycoforms electrophoretic separation, where the CH derivatives are used as dynamic coatings.

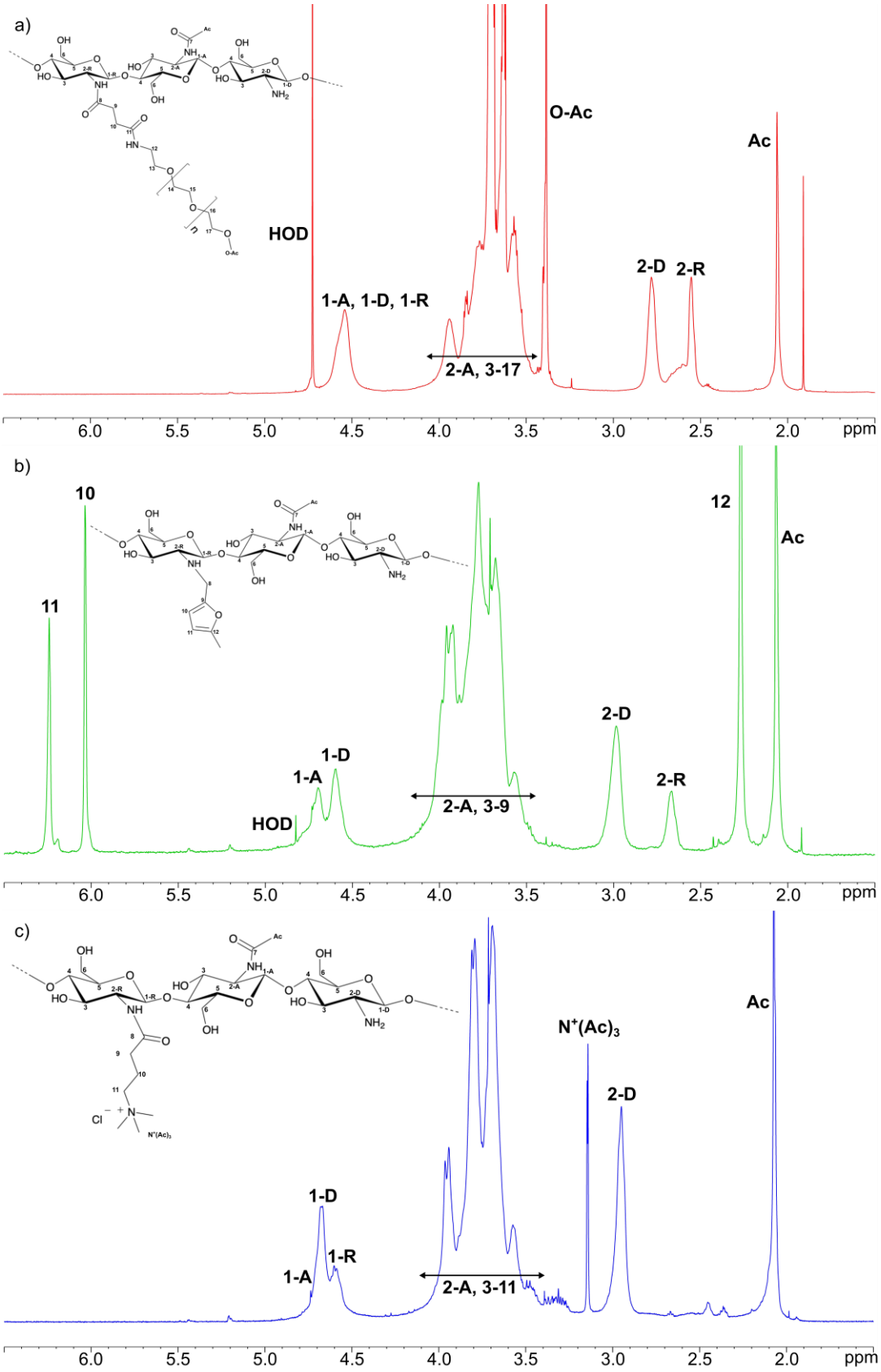

Figure 3. ^{1}H NMR spectra of Ch derivatives in D_2O at 303 K: a) Ch-Ome-PEG, b) Ch-MF and c) Ch-QA.

242

243 **Table 1.** ^{1}H and ^{13}C NMR peaks identification of derivatives.

244

245

		Ch-Ome-PEG	**Ch-MF**	**Ch-QA**
		(ppm)	(ppm)	(ppm)
13C	1-A	104	102.3	102.6
	1-D	104	104.1	102.8
	1-R	104	-	104,1
	2-D	59.1	58.9	58.9
	2-R	33.6	64.2	-
	OAc	60.6	-	-
	$N^{+}(Ac)_3$	-	-	55.7
	Ac	24.8	25.1	24.8
	10	-	108.3	-
	11	-	111.9	-
	12	-	15,5	-
	2-A, 3-17	-	81.4-47	-
	2-A, 3-9	77.3-41.9	-	-
	2-A, 3-11	-	-	81.7-58.2
1H	1-A	4.6	4.7	4.7
	1-D	4.6	4.6	4.7
	1-R	4.6	-	4.6
	2-D	2.7	2.9	2.9
	2-R	2.6	2.7	-
	OAc	3.4	-	-
	$N^{+}(Ac)_3$	-	-	3.2
	Ac	2.05	2.1	2.1
	10	-	6	-
	11	-	6.3	-
	12	-	2.3	-
	2-A, 3-17	4.1-3.6	-	-
	2-A, 3-9	-	4.1-3.6	-
	2-A, 3-11	-	-	4.0-3.6
		Ch-Ome-PEG	**Ch-MF**	**Ch-QA**
	DS (%)	40	22	5

Figure 3 illustrates the results from NMR analysis, which is one of the major methods used for determining the DA for chitosan [41] and DS for its derivatives [42,43]. In Table 1, the chemical shift values were reported. The typical signals of chitosan are present: the peak at around 2 ppm corresponds to the acetyl signal (Ac), the peak at around 3 ppm corresponds to the H2 (2-D) of the deacetylated unit, the peaks in the range 4.0-3.5 ppm correspond to pyranose ring protons and to the H2 (2-A) of the acetylated unit, and the peaks in the range 5.0-4.5 ppm correspond to anomeric signals H1. For all derivatives, in addition to the characteristic peaks of the starting chitosan, the peaks corresponding to the different substituents are present and the attributions were reported in detail in the spectra (Figure 3). The peaks were assigned by HSQC-dept (Figure S1): the peak at around 2 ppm corresponds to the acetyl signal (Ac), the peaks in the range 4.0-3.5 ppm correspond to pyranose ring protons, and the peak at 4.5 ppm corresponds to anomeric signals H1; peaks in the range 2.9-2.6 ppm correspond, respectively to H2, substituted (H2-NHR) and not substituted (H2-D), and to $N^{+}(CH_3)_3$ group of Ch-QA; the peak at 3.4 ppm corresponds to -OCH_3 group of Ch-Ome-PEG. Supportive FTIR analysis is presented in Figure S2. Stokes-Einstein equation allowed the determination of the DS. Ch-Ome-PEG resulted as the derivative more highly substituted with a DS of 40. Ch-MF and Ch-QA have a DS of 22 and 5, respectively. As expected, nucleophilic substitution and amination lead to a higher DS, compared to condensation. The assessment of the Ch derivatives steric hindrance and charges was performed by DLS analysis.

Table 2. Characterization of Ch and its derivatives by DLS and Zp.

Sample	Rh (nm)	MW (kDa)	Zp (mV)
Ch	5.9(±1.8)*	50	+6.1(±0.2)*
Ch-Ome-PEG	10.7(±0.1)**	152	+6.7(±0.2)***
Ch-MF	6.3(±0.6)**	55	+12.8(±0.6)***
Ch-QA	6.1(±0.7)**	52	+49.5(±0.8)***

* in 0.3 M AcONa/0.3 M AcOOH

** in 0.3 M AcONa

*** in water

Table 2 reports the results of DLS and Zp measurements, which are useful to estimate molecular weights and the electrostatic charging of Ch and its derivatives [44]. All the Ch derivatives showed a hydrodynamic radius Rh, which is similar or higher than the pristine Ch, as a result of Ch backbone modification. The analysis revealed a Rh of 10.7 nm (±0.1) for Ch-Ome-PEG, 6.3 nm (±0.6) for Ch-MF and 6.1 nm (±0.7) for Ch-QA, to be compared with 5.9 nm (±1.8) for pristine Ch. Rh measurement enabled the estimation of the derivatives MW, using the Stokes-Einstein equation: the Ch-Ome-PEG, with a MW of 152 kDa, was the heaviest molecule if compared with the other derivatives, Ch-MF (55 kDa) and Ch-QA (52 kDa), which did not substantially differ from pristine Ch (50 kDa). The results obtained for Ch-Ome-PEG were comparable to those obtained using HP-SEC-TDA (Figure S3, Table S1), with an estimated MW of 184 kDa and a hydrodynamic radius of 13 nm. Because of a lack of solubility and interaction with the stationary phase, it was not possible to analyze the Ch-MF and Ch-QA derivatives by HP-SEC-TDA. Based on the results of Zp and MW, Ch-Ome-PEG holds the highest steric hindrance, if compared with Ch-MF and Ch-QA. Higher Rh and MW are related to a higher degree of substitution (Table 1) and by the arrangement of the Ch-Ome-PEG structure, characterized by long chains of CH_2-CH_2-O segments, which affect the derivative 3D conformation.

All three derivatives were soluble in water, differently from pristine Ch, with Zp values ranging from a minimum +6.7 mV (±0.2) for Ch-Ome-PEG to a maximum of +49.5 mV (±0.8) for Ch-QA. Ch-QA

showed a significative increased charge, as expected by the introduction of quaternary ammine functionality onto the Ch polymeric structure. For completeness, Zp of pristine Ch was given in a solution of 0.3 M AcONa/0.3 M AcOOH: however, this value is not directly comparable to those of the derivatives, as the test conditions were different.

The effect on the viscosity of an ideal solution to be applied in CE was investigated through shear stress analysis on Ch derivative solutions, assessing the relationship between the mechanical behavior and chemical properties of biopolymers solutions [45]. The rheological properties were investigated as variation of the viscosity as a function of the shear rate. Preliminary tests performed at different concentrations of pristine Ch (Figure S4) showed, as expected, an increase of viscosity with increasing concentrations, with viscosity remaining independent of the shear rate in the evaluated range. Ch derivatives rheology were also analyzed to understand the difference in rheological properties (Figure S5). In the selected concentration ranges (5 mg/mL), the viscosity of Ch and Ch-QA was constant at about 3 mPa·s, showing a Newtonian liquid behavior; differently, Ch-Ome-PEG and Ch-MF showed a pseudoplastic behavior with the viscosity decreasing at increasing shear rates, within the ranges 1.5-4 mPa·s for Ch-Ome-PEG and 3-4 mPa·s for Ch-MF. Nonetheless, note that Ch derivatives concentrations in the order of ng/mL, as those used for CE tests, did not affect the water solution rheological behavior (data not shown).

To summarize the material characterization, all Ch derivatives were soluble in water after successful modification (with DS reported in Table 1). Ch-MF and Ch-QA showed a Rh around ≈ 6 nm and a MW around 50 kDa, while Ch-Ome-PEG showed a higher Rh and MW (Rh 10.7 nm ±0.1 and MW 152 kDa), having increased steric hindrance. Ch-Ome-PEG and Ch-MF showed weak positive charge with a Zp around ≈ 10 mV, Ch-QA reached a strong positive charge of ≈ 50 mV, due to the presence of quaternary ammonium.

To assess the effect of Ch derivatives as dynamic coatings, they were added to the traditional running buffer for CDT analysis, evaluating both migration times and peak resolution. The goal was to increase the hTf glycoform peak resolution (R), whilst maintaining comparable migration times. Concentrations of Ch derivatives higher than 1 µg/mL were characterized by poor reproducibility (preliminary tests, not reported in the present work); as such, here we presented representative results at a lower concentration, i.e., 100 ng/mL. Additional experiments at different concentrations are reported in the Supplemental Information (Table S2).

Figure 4 shows the obtained electropherograms, with a comparison between the traditional method (i.e., the one described in the "CE analysis" section), where only DAB was used, and the proposed variations, where Ch derivatives were added (in the presence of DAB). All electropherograms showed the characteristic peaks, where immunoglobulins migrated first followed by the different glycoforms of hTf. The traditional method (Figure 4a) allowed the resolution, even if not at baseline level, of the peaks P_2, P_3, P_4 and P_5. Tests performed adding Ch derivatives showed neat differences in peak resolution, particularly between P_2 (disialo-hTf) and P_3 (trisialo-hTf). For all methods, CDT% was assessed at around 13% of total Tf. The methods involving the use of Ch-Ome-PEG (CDT% 13.35%) and Ch-MF (CDT% 13.33 %) show CDT% very close values to the traditional method (CDT% 13.36%).

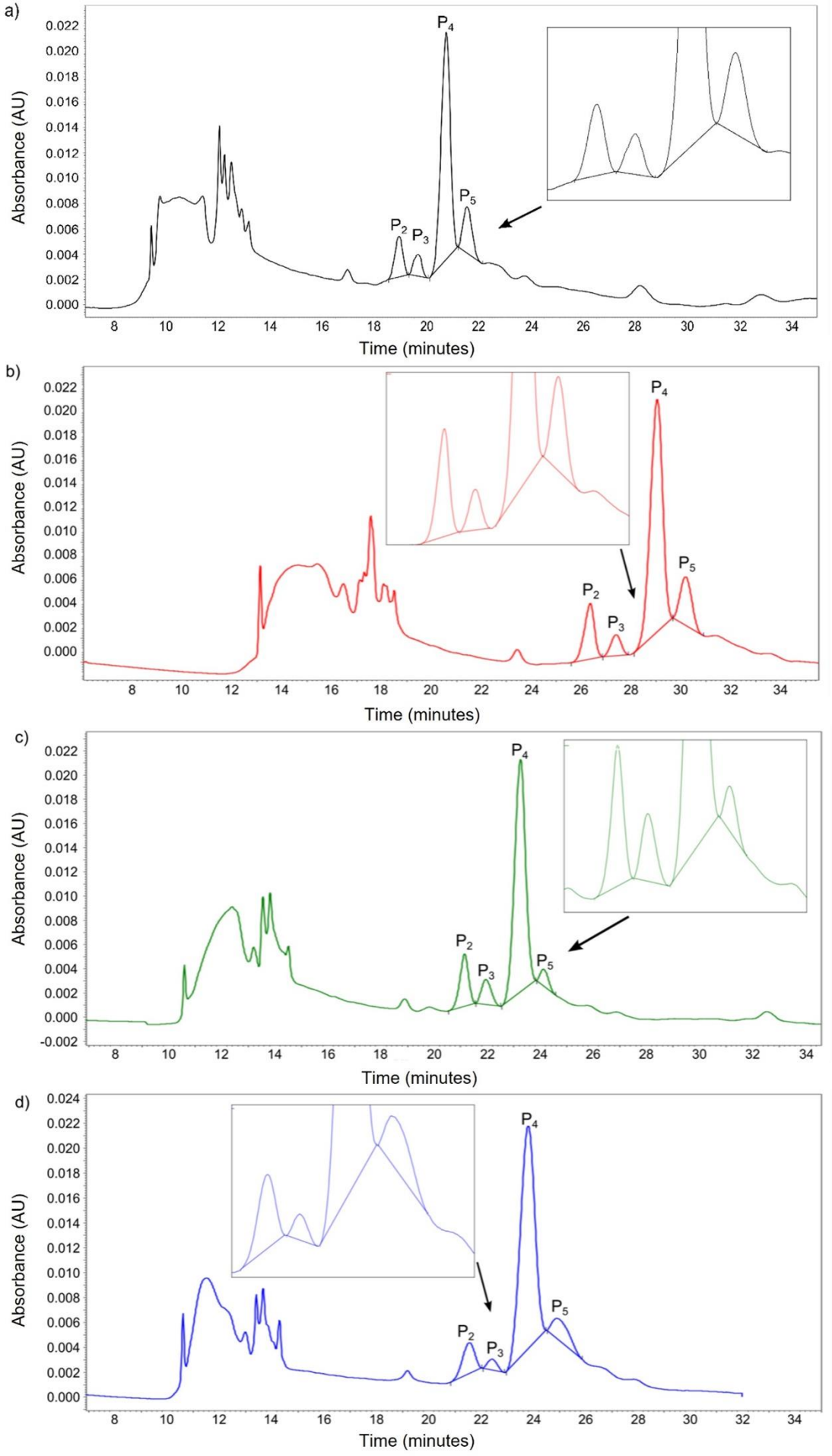

321

Figure 4. Electropherograms obtained from: a) traditional CDT analysis (R= 1.14), (%CDT = 13.36% of total Tf); b) CDT analysis performed with traditional running buffer added with 100 ng/mL Ch-Ome-PEG (R= 1.35), (%CDT = 13.35% of total Tf); c) CDT analysis performed with traditional running buffer added with 100 ng/mL Ch-MF (R= 1.21), (%CDT = 13.33% of total Tf); d) CDT analysis performed with traditional running buffer added with 100 ng/mL Ch-QA (R= 1.10), (%CDT= 9.13% of total Tf). Peaks are numbered as follows: P_2= disialo-hTf; P_3= trisialo-hTf; P_4= tetrasialo-hTf; P_5= pentasialo-hTf. AU = absorbance units at 200 nm wavelength.

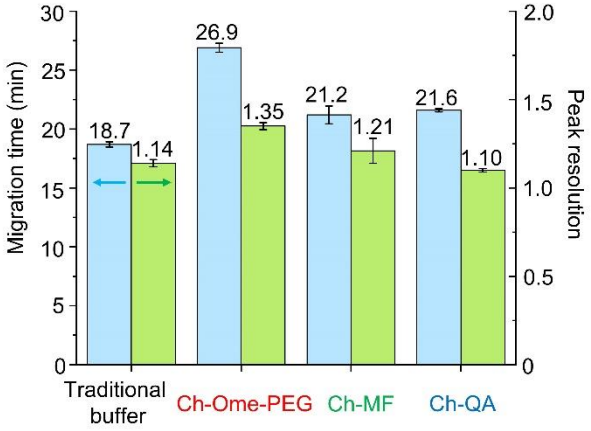

Figure 5. Summary of migration times of disialo-hTf glycoform (blue bar, left y-axis) and peak resolution between disialo-hTf and trisialo-hTf glycoforms (green bar, right axis) and using Ch derivatives as dynamic coatings in capillary electrophoreris, at concentrations equal to 100 ng/mL. Standard deviation was calculated on the base of 5 multiple runs.

Figure 5 summarizes the results of peak resolution between disialo-hTf and trisialo-hTf glycoforms, together with disialo-hTf glycoform migration times. The peak resolution between disialo-hTf and trisialo-hTf glycoforms increased in comparison to the traditional method, when Ch-Ome-PEG and Ch-MF were used. In particular, Ch-Ome-PEG provided the highest resolution (R= 1.35) between disialo- and trisialo-hTf. Under these conditions, the obtained resolution between the two peaks approached the desirable value of R= 1.5. Although Ch-MF addition provided a good resolution between disialo-hTf and trisialo-hTf peaks (R=1.21), this advantage was not reflected in the separation between the tetrasialo-hTf and pentasialo-hTf peaks (Figure 4c), which appear partially overlapped. The use of Ch-QA offered a relatively good resolution (R=1.10), which however was not higher than that obtained with the traditional buffer; also, it was characterized by a broadening of peaks P4 and P5, probably due to spurious interactions with the capillary wall. All experiments performed with Ch derivatives determined an overall increase of migration times, suggesting a decrease of the velocity of the EOF. Although the increase of migration times is generally undesirable, as it impacts the overall analysis time, the observed increase could be accepted since it was positively counterbalanced by resolution improvements. To estimate the degree of ionic interactions at the capillary wall, a condition generating the EOF, the streaming potential (SP) was measured prior to every set of separations with each running buffer composition. In brief, SP is an electric potential difference generated between the two ends of a fused-silica capillary, when an electrolyte is pumped through it. It is dependent on solution viscosity, ionic diffusivity, electric constant, zeta potential, and hydrodynamic radius, i.e., factors also affecting EOF. Results (Table S3) show that SP values measured in the presence of the Ch derivatives slightly change from the traditional running buffer, with Ch-Ome-PEG showing the highest value and the highest migration times.

In terms of separation improvements, Ch-Ome-PEG proved to be the most promising additive, offering the highest increase of resolution. Considering the physico-chemical characterization of the derivatives, this effect could be related to the high steric hindrance (determined by DLS and HP-SEC analysis), which may provide a better shielding of the capillary wall from the adsorption of macromolecules, such as hTf.

Furthermore, we speculate that the long chains of Ome-PEG may have created higher restriction to the mobility of the hTf glycoforms, thus reducing the random changes of conformation of the macromolecules and consequently their inhomogeneity. Although the improvement in separation compared to the traditional method could seem relatively small, we were able to prove that modified chitosan-based dynamic coatings may have a positive effect on the separation of hTf glycofoms, demonstrating their ability to shield the capillary surface from interactions with macromolecules. However, further optimization and validation of the method using chitosan-based dynamic coating is necessary to propose this additive in a new analytical CE method.

While most of the current routine CE methods for CDT analysis typically adopt fused-silica capillaries with an inner diameter of 25-30 µm, to reduce peak broadening, in the present work, a 50 µm diameter capillary was used to limit the issues arising when applying solutions with very different viscosity. An improvement of the peak sharpness is, hence, expected adopting thinner capillaries for the development of a new CE method which implies the use of derivatized chitosan. In Figure 6, an electropherogram of hTf conducted in a 30 µm i.d. capillary using a running buffer containing 100 ng/mL Ch-Ome-PEG is illustrated. Although not specifically optimized, the use of a smaller capillary diameter provided am even better resolution (i.e., R= 1.49), in comparison to the 50 µm i.d. capillary, with the separation of the two peaks of interest almost at the baseline. This strongly suggests further benefits from the adoption of Ch derivatives for the development of a new optimized method for CDT analysis.

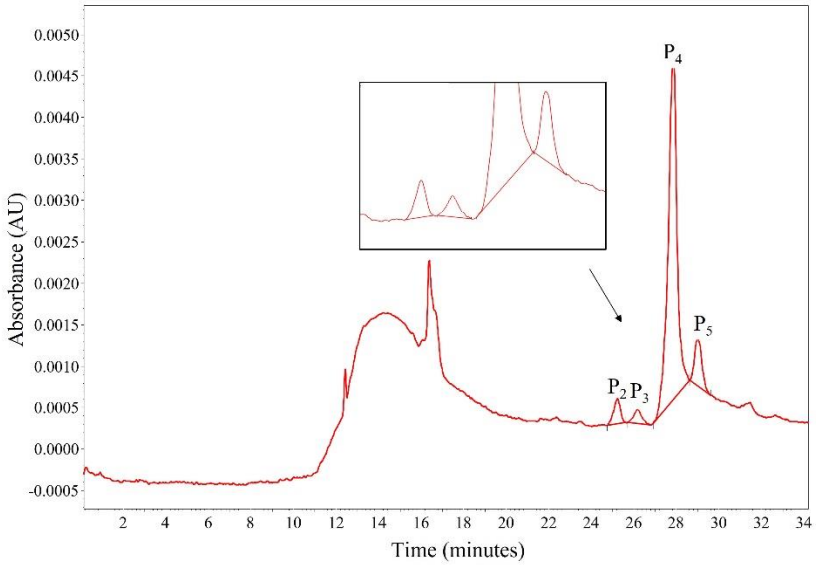

Figure 6. Electropherogram obtained from CDT analysis performed with traditional running buffer added with 100 ng/mL Ch-Ome-PEG (R= 1.49) (CDT % = 4.5%, of total Tf) in a capillary with 30 µm i.d. and 30 kV separation voltage. Peaks are numbered as follows: P_2= disialo-hTf; P_3= trisialo-hTf; P_4= tetrasialo-hTf; P_5= pentasialo-hTf. AU = absorbance units at 200 nm wavelength.

CONCLUSIONS

In conclusion, the present study was focused on the preparation and characterization of water-soluble derivatives of chitosan, an abundant polysaccharide, and on the preliminary assessment of their use as dynamic coatings for CE separation of macromolecules. Specifically, we tested the use chitosan

derivatives for human transferrin separation, in order to improve peak resolution of one of its glycoforms, i.e. CDT, a typical biomarker of chronic alcohol abuse.

Chitosan has been modified successfully via three reactions, using nucleophilic substitution, reductive amination, and condensation. The results have shown that the type of modifications introduced in the chitosan molecule have distinct influence on the resolution of the hTf glycoforms, being Ch-Ome-PEG the most promising additive. Future studies will be needed to achieve proper optimization and validation of the proposed method for CDT analysis. Although more work should be done in this direction, the present study may open the way to a new class of dynamic coating agents to be adopted in CE, where the problem of hindering the adsorption of the analytes on the capillary walls is still an open issue. As an additional perspective, in future, we envision the use of modified chitosans as dynamic coatings for other applications, e.g. the CE separation of DNA fragments and drugs. Considering the chiral nature of Ch, its potential could also be tested with enantiomeric species.

SUPPORTING INFORMATON

HSQC-dept spectra, HP-SEC-TDA of Ch-Ome-PEG and Ch, Rheology: viscosity behavior of Ch at different concentration, Capillary Electrophoresis: peak resolution results and migration times using Ch derivatives as dynamic coating at different concentrations (PDF).

AUTHOR INFORMATION

Corresponding Authors

Franco Tagliaro - Unit of Forensic Medicine, Department of Diagnostics and Public Health, University of Verona, Verona, Italy. Orcid: 0000-0002-2187-9128 Email: franco.tagliaro@univr.it

Carlo Antonini - Department of Materials Science, University of Milano - Bicocca, Milano, 20125 Milan, Italy; Telephone number Orcid: 0000-0002-4975-4001 Email: carlo.antonini@unimib.it

Sabrina Bertini - Istituto di Ricerche Chimiche e Biochimiche G. Ronzoni, Carbohydrate Science Department, 20133 Milan, Italy Orcid: 0000-0003-1714-5823 Email: bertini@ronzoni.it

Author Contributions

‡NP investigation, methodology, conceptualization, writing-original draft, writing-original draft. ‡IT conceptualization, writing-original draft, writing-review and editing. BP investigation, writing-review and editing. AA investigation, methodology, conceptualization, writing-review and editing. FT conceptualization, supervision, writing-review and editing. CA conceptualization, supervision, writing-review and editing. LR conceptualization, writing-review and editing. FC Investigation. GM Methodology. SB conceptualization, supervision, writing-review and editing.

‡These authors contributed equally. All authors have read and agreed to the published version of the manuscript.

Funding

This work was in part financed in terms of personnel costs by the Ministry of Science and Higher Education of the Russian Federation within the framework of state support for the creation and development of World-Class Research Centres "Digital Biodesign and personalized healthcare" N° 075-15-2020-926.

Data Availability Statement

The data that support the findings of this study are available from the corresponding author upon reasonable request.

Conflicts of Interest

The authors declare no conflict of interest.

ACKNOWLEDGMENT

C.A. acknowledges partial support from the Italian Ministry for University and Research (MIUR) through the Rita Levi Montalcini fellowship for young researchers. S.B., A.A, and B.P. acknowledge technical support by Cesare Cosentino and Michela Parafioriti for NMR analyses and Edwin Yates for Writing-review and editing.

REFERENCES

[1] M. Mabrouk, S.F. Hammad, F.R. Mansour, A.A. Abdella, A Critical Review of Analytical Applications of Chitosan as a Sustainable Chemical with Functions Galore, Crit Rev Anal Chem. (2022). https://doi.org/10.1080/10408347.2022.2099220.

[2] L. Casettari, D. Vllasaliu, E. Castagnino, S. Stolnik, S. Howdle, L. Illum, PEGylated chitosan derivatives: Synthesis, characterizations and pharmaceutical applications, Prog Polym Sci. 37 (2012) 659–685. https://doi.org/10.1016/j.progpolymsci.2011.10.001.

[3] J.C.V. Ribeiro, R.S. Vieira, I.M. Melo, V.M.A. Araújo, V. Lima, Versatility of Chitosan-Based Biomaterials and Their Use as Scaffolds for Tissue Regeneration, Scientific World Journal. 2017 (2017). https://doi.org/10.1155/2017/8639898.

[4] P. Sahariah, M. Másson, Antimicrobial Chitosan and Chitosan Derivatives: A Review of the Structure-Activity Relationship, Biomacromolecules. 18 (2017) 3846–3868. https://doi.org/10.1021/acs.biomac.7b01058.

[5] M.M. Jaworska, D. Antos, A. Górak, Review on the application of chitin and chitosan in chromatography, React Funct Polym. 152 (2020). https://doi.org/10.1016/j.reactfunctpolym.2020.104606.

[6] A.C. Sadiq, A. Olasupo, W.S.W. Ngah, N.Y. Rahim, F.B.M. Suah, A decade development in the application of chitosan-based materials for dye adsorption: A short review, Int J Biol Macromol. 191 (2021) 1151–1163. https://doi.org/10.1016/j.ijbiomac.2021.09.179.

[7] X. qi Liu, X. xin Zhao, Y. Liu, T. an Zhang, Review on preparation and adsorption properties of chitosan and chitosan composites, Polymer Bulletin. 79 (2022) 2633–2665. https://doi.org/10.1007/s00289-021-03626-9.

[8] Y.L. Nunes, F.L. de Menezes, I.G. de Sousa, A.L.G. Cavalcante, F.T.T. Cavalcante, K. da Silva Moreira, A.L.B. de Oliveira, G.F. Mota, J.E. da Silva Souza, I.R. de Aguiar Falcão, T.G. Rocha, R.B.R. Valério, P.B.A. Fechine, M.C.M. de Souza, J.C.S. dos Santos, Chemical and physical Chitosan modification for designing enzymatic industrial biocatalysts: How to choose the best strategy?, Int J Biol Macromol. 181 (2021) 1124–1170. https://doi.org/10.1016/j.ijbiomac.2021.04.004.

[9] E.S. Ribeiro, B.S. de Farias, T.R. Sant'Anna Cadaval Junior, L.A. de Almeida Pinto, P.S. Diaz, Chitosan–based nanofibers for enzyme immobilization, Int J Biol Macromol. 183 (2021) 1959–1970. https://doi.org/10.1016/j.ijbiomac.2021.05.214.

[10] J.J. Thevarajah, M.P. van Leeuwen, H. Cottet, P. Castignolles, M. Gaborieau, Determination of the distributions of degrees of acetylation of chitosan, Int J Biol Macromol. 95 (2017) 40–48. https://doi.org/10.1016/j.ijbiomac.2016.10.056.

[11] S. Štěpánová, V. Kašička, Recent applications of capillary electromigration methods to separation and analysis of proteins, Anal Chim Acta. 933 (2016) 23–42. https://doi.org/10.1016/j.aca.2016.06.006.

[12] C.E. Evans, A.M. Stalcup, Comprehensive strategy for chiral separations using sulfated cyclodextrins in capillary electrophoresis, in: Chirality: The Pharmacological, Biological, and Chemical Consequences of Molecular Asymmetry, Wiley Online Library, 2003: pp. 709–723.

[13] D.C. Harris, Quantitative chemical analysis, Macmillan, 2010.

[14] A.C. Moffat, M.D. Osselton, B. Widdop, J. Watts, Clarke's analysis of drugs and poisons, Pharmaceutical press London, 2011.

[15] J. Frenz, W.S. Hancock, High performance capillary electrophoresis, Trends Biotechnol. 9 (1991) 243–250.

[16] W. Thormann, S. Molteni, J. Caslavska, A. Schmutz, Clinical and forensic applications of capillary electrophoresis, Electrophoresis. 15 (1994) 3–12.

[17] S.N. Krylov, D.A. Starke, E.A. Arriaga, Z. Zhang, N.W.C. Chan, M.M. Palcic, N.J. Dovichi, Instrumentation for chemical cytometry, Anal Chem. 72 (2000) 872–877. https://doi.org/10.1021/ac991096m.

[18] C. Malburet, L. Leclercq, J.F. Cotte, J. Thiebaud, H. Cottet, Study of Interactions between Antigens and Polymeric Adjuvants in Vaccines by Frontal Analysis Continuous Capillary Electrophoresis, Biomacromolecules. 21 (2020) 3364–3373. https://doi.org/10.1021/acs.biomac.0c00782.

[19] J. Wang, Z. Zhu, X. Wang, L. Yang, L. Liu, J. Wang, E. Igbinigie, X. Liu, J. Li, L. Qiu, Y.Q. Li, P. Jiang, A novel monitoring approach of antibody-peptide binding using "bending" capillary electrophoresis, Int J Biol Macromol. 113 (2018) 900–906. https://doi.org/10.1016/j.ijbiomac.2018.03.032.

[20] B. Coulter, Introduction to capillary electrophoresis, 1991.

[21] V. Dolník, Capillary electrophoresis of proteins 2005-2007, Electrophoresis. 29 (2008) 143–156. https://doi.org/10.1002/elps.200700584.

[22] L.P. Zhou, Y. Chen, H. Hu, B. Yu, G.W. Wang, H.L. Cong, Novel diazoresin/carboxymethyl chitosan capillary coating for the analysis of proteins by capillary electrophoresis, Ferroelectrics. 529 (2018) 24–32. https://doi.org/10.1080/00150193.2018.1448184.

[23] X. Huang, Q. Wang, B. Huang, Preparation and evaluation of stable coating for capillary electrophoresis using coupled chitosan as coated modifier, in: Talanta, Elsevier, 2006: pp. 463–468. https://doi.org/10.1016/j.talanta.2005.10.015.

[24] M. Herrero, J. Bernal, D. Velasco, C. Elvira, A. Cifuentes, Connections between structure and performance of four cationic copolymers used as physically adsorbed coatings in capillary electrophoresis, J Chromatogr A. 1217 (2010) 7586–7592. https://doi.org/10.1016/j.chroma.2010.09.063.

[25] S. Olmo, R. Gotti, M. Naldi, V. Andrisano, N. Calonghi, C. Parolin, L. Masotti, V. Cavrini, Analysis of human histone H4 by capillary electrophoresis in a pullulan-coated capillary, LC-ESI-MS and MALDI-TOF-MS, Anal Bioanal Chem. 390 (2008) 1881–1888. https://doi.org/10.1007/s00216-008-1903-5.

[26] P. Sun, A. Landman, R.A. Hartwick, Chitosan Coated Capillary with Reversed Electroosmotic Flow in Capillary Electrophoresis for the Separation of Basic Drugs and Proteins, Journal of Microcolumn Separation. 6 (1994) 403–407.

[27] Y.J. Yao, S.F.Y. Li, Capillary zone electrophoresis of basic proteins with chitosan as a capillary modifier, J Chromatogr A. 663 (1994) 97–104.

[28] T. Takayanagi, S. Motomizu, Chitosan as Cationic Polyelectrolyte for the Modification of Electroosmotic Flow and Its Utilization for the Separation of Inorganic Anions by Capillary Zone Electrophoresis, Analytical Sciences. 22 (2006) 1241–1243.

[29] X. Fu, L. Huang, F. Gao, W. Li, N. Pang, M. Zhai, H. Liu, M. Wu, Carboxymethyl chitosan-coated capillary and its application in CE of proteins, Electrophoresis. 28 (2007) 1958–1963. https://doi.org/10.1002/elps.200600558.

[30] Y. Liu, X. Fu, Y. Bai, M. Zhai, Y. Liao, J. Liao, H. Liu, Improvement of reproducibility and sensitivity of CE analysis by using the capillary coated dynamically with carboxymethyl chitosan, Anal Bioanal Chem. 399 (2011) 2821–2829. https://doi.org/10.1007/s00216-011-4659-2.

[31] Y. Jia, J. Cao, J. Zhou, P. Zhou, Methyl chitosan coating for glycoform analysis of glycoproteins by capillary electrophoresis, Electrophoresis. 41 (2020) 729–734. https://doi.org/10.1002/elps.201900333.

[32] N.M. Porpiglia, S.A. Savchuk, S.A. Appolonova, F. Bortolotti, F. Tagliaro, Capillary Electrophoresis (CE) vs. HPLC in the determination of asialo-Tf, a crucial marker for the reliable interpretation of questioned CDT increases, Clinica Chimica Acta. 486 (2018) 49–53.

[33] V. Paterlini, N.M. Porpiglia, E.F. de Palo, F. Tagliaro, Asialo-transferrin: Biochemical aspects and association with alcohol abuse investigation, Alcohol. 78 (2019) 43–50. https://doi.org/10.1016/j.alcohol.2019.03.002.

[34] F.C. Chang, C.T. Tsao, A. Lin, M. Zhang, S.L. Levengood, M. Zhang, PEG-chitosan hydrogel with tunable stiffness for study of drug response of breast cancer cells, Polymers (Basel). 8 (2016). https://doi.org/10.3390/polym8040112.

[35] F. Crivellente, G. Fracasso, R. Valentini, G. Manetto, A.P. Riviera, F. Tagliaro, Improved method for carbohydrate-deficient transferrin determination in human serum by capillary zone electrophoresis, J Chromatogr B Biomed Sci Appl. 739 (2000) 81–93.

[36] R.P. Oda, R. Prasad, R.L. Stout, D. Coffin, W.P. Patton, D.L. Kraft, J.F. O'Brien, J.P. Landers, Capillary electrophoresis-based separation of transferrin sialoforms in patients with carbohydrate-deficient glycoprotein syndrome, Electrophoresis. 18 (1997) 1819–1826.

[37] R. Prasad, R.L. Stout, D. Coffin, J. Smith, Analysis of carbohydrate deficient transferrin by capillary zone electrophoresis, Electrophoresis. 18 (1997) 1814–1818.

[38] H. Stibler, Carbohydrate-deficient transferrin in serum: a new marker of potentially harmful alcohol consumption reviewed, Clin Chem. 37 (1991) 2029–2037.

[39] C.H. Yang, S.H. Chen, Y.W. Pan, C.N. Chuang, W.C. Chao, T.H. Young, W.Y. Chiu, C.K. Wang, K.H. Hsieh, Preparation and characterization of methoxy-poly(ethylene glycol) side chain grafted onto chitosan as a wound dressing film, J Appl Polym Sci. 132 (2015). https://doi.org/10.1002/app.42340.

[40] S. Magli, G.B. Rossi, G. Risi, S. Bertini, C. Cosentino, L. Crippa, E. Ballarini, G. Cavaletti, L. Piazza, E. Masseroni, F. Nicotra, L. Russo, Design and Synthesis of Chitosan—Gelatin Hybrid Hydrogels for 3D Printable in vitro Models, Front Chem. 8 (2020). https://doi.org/10.3389/fchem.2020.00524.

[41] E. Fernandez-Megia, R. Novoa-Carballal, E. Quiñoá, R. Riguera, Optimal routine conditions for the determination of the degree of acetylation of chitosan by 1H-NMR, Carbohydr Polym. 61 (2005) 155–161. https://doi.org/10.1016/j.carbpol.2005.04.006.

[42] S. Magli, L. Rossi, C. Consentino, S. Bertini, F. Nicotra, L. Russo, Combined analytical approaches to standardize and characterize biomaterials formulations: application to chitosan-gelatin cross-linked hydrogels, Biomolecules. 11 (2021) 683.

[43] I. Donati, S. Stredanska, G. Silvestrini, A. Vetere, P. Marcon, E. Marsich, P. Mozetic, A. Gamini, S. Paoletti, F. Vittur, The aggregation of pig articular chondrocyte and synthesis of extracellular matrix by a lactose-modified chitosan, Biomaterials. 26 (2005) 987–998. https://doi.org/10.1016/j.biomaterials.2004.04.015.

[44] J. Jiang, G. Oberdörster, P. Biswas, Characterization of size, surface charge, and agglomeration state of nanoparticle dispersions for toxicological studies, Journal of Nanoparticle Research. 11 (2009) 77–89. https://doi.org/10.1007/s11051-008-9446-4.

[45] Y. Jia, J. Cao, J. Zhou, P. Zhou, Methyl chitosan coating for glycoform analysis of glycoproteins by capillary electrophoresis, Electrophoresis. 41 (2020) 729–734. https://doi.org/10.1002/elps.201900333.

TABLE OF CONTENTS